Journal of Power Sources 187 (2009) 452–460

Contents lists available at ScienceDirect

Journal of Power Sources

journal homepage: www.elsevier.com/locate/jpowsour

On the intrinsic transient capability and limitations of solid oxide fuel cell systems

Fabian Mueller*, Faryar Jabbari, Jacob Brouwer

National Fuel Cell Research Center, University of California, Irvine, CA 92697, United States

ARTICLE INFO

Article history:
Received 16 September 2008
Received in revised form 5 November 2008
Accepted 6 November 2008
Available online 24 November 2008

Keywords:
Solid oxide fuel cell
Transient capability
Controls
Performance limitation
Non-dimensional analysis

ABSTRACT

The intrinsic transient performance capability and limitation of integrated solid oxide fuel cell (SOFC) systems is evaluated based on the system balance-of-plant response and fuel cell operating requirements (i.e., allowable deviation from nominal operation). Specifically, non-dimensional relations are derived from conservation principles that quantify the maximum instantaneous current increase that a solid oxide fuel cell system can safely manage based on (1) the desired fuel cell operating point, (2) the maximum allowable fuel utilization, (3) the maximum average fuel cell temperature deviation, (4) the response delay and (5) the operating requirements of the system balance-of-plant components. New non-dimensional numbers representing the ratio of species or thermal convection to volumetric capacitance in the fuel cell during balance-of-plant delay have been developed.

The analyses indicate: (1) SOFC intrinsic transient performance is largely limited by fuel processor flow delays that can cause fuel depletion in the anode compartment and (2) that with proper system actuators and control design transient operation of SOFC systems should be possible while maintaining SOFC average temperature within a degree. The SOFC system fuel processor lag appears to be the cause of SOFC load following limitation, while lag in air handling appears to be manageable. To demonstrate methods to avoid fuel depletion limitation a fuel flow lead compensator is developed. Integrated system simulations with proper control demonstrate significant SOFC transient performance within fuel cell operating requirements.

1. Introduction

Significant changes in electrical power generation are required to address the environmental pollutant and greenhouse gas emissions challenges, while meeting ever increasing electricity demands. Solid oxide fuel cell (SOFC) systems are an attractive, emerging technology for electrical power generation. Solid oxide fuel cells directly convert fuel to electricity. The direct conversion of fuel allows for high fuel to electric conversion efficiencies (even at small scales) with minimal pollutant emissions [1]. SOFC technology is being developed by power companies with support from government programs and university research [2–6]. As a result of this research and development, primarily focused on cost reduction, materials, durability, and systems integration, cost competitive integrated SOFC systems are becoming apparent.

However, limited research has been conducted to understand and improve SOFC system transient load following capabilities. Transient SOFC operation could allow stand-alone system installations with reduced energy storage (e.g., capacitors, batteries) equipment requirements and costs. Further, SOFC systems with transient load following can better support the electrical grid and meet the dynamic loads of off-grid applications. The development of SOFC system transient load following will thus increase the attractiveness and market potential of SOFC technology. Yet to-date SOFC systems have typically been operated conservatively as steady-state base-loaded generators. This is partially due to the misperception of SOFC technology fragility and/or vulnerability to transient operation and to the desire of manufacturers to demonstrate system longevity. Steady-state SOFC system operation has also been the norm due to the lack of sufficient understanding and controls for enabling system transient response while maintaining all SOFC operating requirements.

Solid oxide fuel cells are electrochemical generators that directly convert fuel and oxygen to electricity. If electrochemically reactive species are available at reaction sites (triple phase boundaries) during operating conditions, the SOFC can respond to load variations on the time scale of the electrochemistry (order of milliseconds) [7]. Following a load variation or disturbance, the challenge is to manipulate the balance-of-plant components (including turbomachinery, blowers, fuel valves, heat exchanger bypass valves, small combustors, etc.) so as to maintain the fuel cell and other system components within operating requirements. Control systems

* Corresponding author. Tel.: +1 949 824 1999; fax: +1 949 824 7423.
E-mail addresses: fm@nfcrc.uci.edu (F. Mueller), fjabbari@uci.edu (F. Jabbari), jb@nfcrc.uci.edu (J. Brouwer).

0378-7753/$ – see front matter © 2008 Elsevier B.V. All rights reserved.
doi:10.1016/j.jpowsour.2008.11.057

Nomenclature

C	specific heat [J kg^{-1} K^{-1}]
d	control demand value
F	Faradays constant [96,485 C mol^{-1}]
h	enthalpy [J mol^{-1}]
i	fuel cell current [A] and integral feedback gain
K	proportional feedback gain
m	mass [kg]
n	number of participating electrons in reaction
N	molar capacity [mol]
$\dot{N}$	molar flow rate [mol s^{-1}]
P	pressure [Pa] and power delay time constant [s]
r	ratio of utilization and control reference value
R	universal gas constant [8.314 J mol^{-1} K^{-1}] and reaction rate [mol s^{-1}] and resistance [ohm]
t	time [s]
T	temperature [K]
u	system input
U	utilization
V	voltage [V] and volume [m^3]
X	mole fraction
y	system output

Greek symbols

τ	time constant [s]
Θ	non-dimensional temperature
Φ	current ratio
Ψ	non-dimensional voltage lost

development must consider that the fuel cell and balance-of-plant components have various characteristic response times.

2. Background

Seven primary SOFC subsystem components are generally required in SOFC systems (as shown in Fig. 1).

(1) The fuel cell to convert the chemical potential between fuel and air to an electric potential. The fuel cell is the heart of the system with the other components supporting its operation.
(2) A fuel control valve to vary the system fuel flow rate to maintain fuel utilization and system operating conditions at part load conditions [8].
(3) A fuel preparation unit to preheat fuel and process (e.g., reform, and/or clean) fuel before the fuel cell.
(4) An air supply unit (e.g., blower) to provide air to the fuel cell for electrochemistry and cooling.
(5) An air preheat unit such that the inlet air is sufficiently hot to maintain fuel cell temperature and temperature gradients within operating constraints.

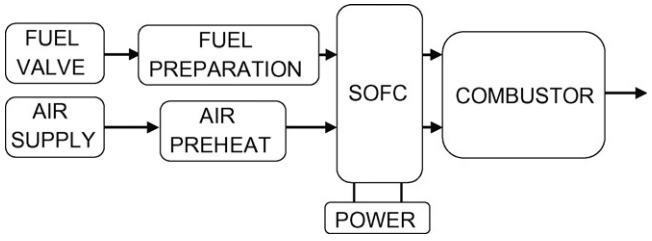

Fig. 1. SOFC stack and required subsystems.

(6) A combustor to oxidize unutilized fuel from the fuel cell, since the fuel cell cannot electrochemically utilize 100% of the fuel.
(7) A power conditioning unit to control the amount of current drawn from the fuel cell and to process (e.g., invert) the current generated for distribution or end-use.

During operation it is critical that (1) sufficient fuel is maintained within the fuel cell anode compartment to support electrochemical reaction and to avoid electrode oxidation (see [9–12]) and (2) fuel cell temperatures are maintained within acceptable limits to support high efficiency operation, reduce thermal fatigue and improve fuel cell durability (see [9,10,13–15]). If any of the system operating requirements cannot be safely maintained during load transients, the rapid fuel cell response must be limited to ensure overall safe system operation [7,9,12,16].

For example, following a load transient (1) the small amount of excess fuel within the fuel cell can become depleted during fuel processor transient operation and (2) the amount of heat generated within the fuel cell varies, potentially causing large temperature variations if the heat cannot be affectively removed from the fuel cell (generally by increasing the air flow rate). Therefore, it may be necessary to limit the fuel cell current to maintain sufficient fuel within the anode compartment and to avoid thermal fatigue in the fuel cell.

Fuel cell fuel depletion and temperature deviation from desired conditions represent two challenging SOFC load following limitations and will be considered in detail here. Of course, special consideration must be given to maintain reasonable combustor and reformer temperatures during transients as well (see [7,17,18]). However, prior research has indicated combustor and reformer temperatures can be maintained and controlled during transients without the need to limit fuel cell load following capability with careful input–output pairing and control (see [7,18]). This is partially due to the fact that the combustor and reformer temperature do not have to be as closely controlled as the fuel cell temperature.

Control concepts have been developed to maintain the fuel cell within operating constraints at steady state (for example see Inui et al. [13]), and several base-loaded SOFC systems have been effectively demonstrated (for example see [5,6,19]). However, SOFC intrinsic load following is not well understood or quantified and controls to enable safe SOFC load following capability need to be developed.

3. Non-dimensional analysis

A non-dimensional analysis was conducted to provide insight into the extent that the fuel cell electrochemical response has to be limited due to a lag in fuel and air actuation. As long as the fuel cell remains within required operating conditions during transient operation, then the fuel cell transient capability does not have to be limited. The analysis is simplified but provides insight into the intrinsic load following capability of SOFC systems based upon a given maximum fuel cell fuel utilization, maximum fuel cell temperature deviation, and performance characteristics of the fuel and air handling components. Both fuel depletion and temperature deviation are investigated individually.

3.1. Fuel depletion

A non-dimensional equation is developed to quantify the maximum current step increase such that fuel utilization never exceeds a maximum. The approach is to non-dimensionalize the fuel cell species conservation equation, assuming a pure (zero-order) fuel processor delay. From the differential equation it is then possible to solve for maximum current increase to maintain the fuel utilization

below the maximum. The following highly simplifying assumptions are made in this analysis:

1) Pure zero-order fuel actuation delay to the fuel cell. Typically the fuel actuator and fuel processor delay will not be zero-order (as will be discussed later), but the zero-order fuel and air delay allow for a simple solution form that is conservative.
2) Hydrogen is the only electrochemically active species.
3) Hydrogen concentrations do not vary across the width and breadth of the fuel cell anode compartment.
4) Constant temperature and pressure.
5) All gases are ideal gases.

These assumptions are made so that a very simple closed form equation for the maximum allowed current increase to avoid fuel depletion while maintaining a maximum temperature deviation can be obtained.

The initial condition is pure hydrogen fuel cell operation at steady state at a given fuel utilization (U). At time $t = 0+$ the current is instantaneously increased to a constant higher value. The fuel cell inlet flow rate required to maintain a constant fuel utilization is delayed by a given amount of time ($t = \tau_{ref}$). During the delay, the amount of fuel within the fuel cell decreases as the electrochemical fuel consumption increases without an increase in anode compartment fuel flow. Once the fuel reaches the fuel cell, the operating utilization is re-established. The critical time is that between the load increase and the fuel cell realization of the fuel flow increase ($0+ < t < \tau_{ref}$). During this time the fuel cell anode fuel mass conservation equation can be written as:

$$N\frac{dX_{out}}{dt} = \dot{N}_{fc}(X_{in} - X_{out}) - \frac{i}{nF} \quad (1)$$

where the number of moles in the pure hydrogen electrochemistry is conserved and fuel consumption is quantified by Faraday's law. In the equation N is the molar capacity in the fuel cell anode, X_{in} is the anode inlet hydrogen mole fraction, X_{out} is the anode outlet hydrogen mole fraction, and $\dot{N}_{fc}$ is the fuel cell anode inlet molar fuel flow rate. Note that following the current increase and during the flow delay ($0+ < t < \tau_{ref}$), the current and fuel flow are both constant. The mass conservation equation makes it possible to analyze the amount of hydrogen within the fuel cell during the flow delay.

To generalize, the conservation equation can be non-dimensionalized using the following non-dimensional parameters:

$$\bar{t} = \frac{t}{\tau_{ref}}, \qquad \bar{U} = \frac{i_\alpha}{\dot{N}_{fc}nF}, \qquad \Phi = \frac{i}{i_\alpha}, \qquad \mathrm{Mu} = \frac{\tau_{ref}i_\alpha}{\bar{U}NnF} \quad (2)$$

where $\bar{t}$ is non-dimensional time based upon τ_{ref} the fuel cell zero-order fuel flow delay, $\bar{U}$ is the reference utilization, i_α the initial current and Mu is a new non-dimensional number, representing the ratio of total number of hydrogen moles flowing into the fuel cell during the fuel flow delay to the fuel cell anode compartment molar capacity. Eq. (1) becomes:

$$\frac{dX_{out}}{d\bar{t}} = \mathrm{Mu}(X_{in} - X_{out} - \Phi\bar{U}) \quad (3)$$

During the fuel delay, $\bar{U}$ is equal to the initial fuel utilization. In a pure hydrogen fuel cell, the initial exit fuel mole fraction is equal to one minus the initial utilization $X_{out}(\bar{t} = 0) = 1 - U_o = 1 - \bar{U}$. With the initial condition, the non-dimensional ordinary differential equation can be solved for an instantaneous current increase in a pure hydrogen fuel cell (i.e., $X_{in} = 1$) during the time of the flow delay:

$$X_{out} = \bar{U}(\Phi - 1)\ \exp(-\mathrm{Mu}\,\bar{t}) - \Phi\bar{U} + 1 \quad (4)$$

Since the maximum fuel utilization will take place at the very moment that the fuel flow increase is realized in the fuel cell anode compartment ($\bar{t} = 1$), the maximum allowable current increase (Φ) for maintaining fuel utilization below a maximum (U_{max}) is determined by solving the above equation for Φ with $X_{out} = 1 - U_{max}$ and $\bar{t} = 1$.

$$\Phi = \frac{r\exp(\mathrm{Mu}) - 1}{\exp(\mathrm{Mu}) - 1} \quad (5)$$

where $r = U_{max}/\bar{U}$ is the ratio of maximum allowable utilization to the initial fuel utilization.

Eq. (5) represents the extent to which fuel cell current can be changed in a pure hydrogen fuel cell so that fuel utilization is maintained below a maximum during the time of a zero-order flow delay. Eq. (5) shows that the extent that the current can be increased depends upon the amount the utilization is allowed to change (r) and the non-dimensional number Mu. Mu captures the affects of the initial fuel utilization, initial operating current, reformer flow delay, and anode compartment molar capacity on fuel cell fuel depletion limitations.

3.2. Temperature deviation

Similar to the fuel depletion analysis, it is possible to develop a non-dimensional relation that quantifies the maximum current increase that is allowed while continuously maintaining average fuel cell temperature deviation below a maximum level. The approach is to non-dimensionalize the fuel cell energy conservation equation, assuming a current step increase, and air manipulation to maintain a constant fuel cell average temperature. From the non-dimensional conservation equation it is then possible to determine the maximum current increase required to maintain a maximum fuel cell temperature deviation during a zero-order flow delay. Again we propose simplifying assumptions to elucidate the intrinsic features of the temperature deviation constraint as follows:

1) Pure zero-order air actuation delay.
2) Concentrations do not vary across the width and breadth of the cathode compartment.
3) The fuel cell is cooled only by air flow through the fuel cell. The cooling provided by heating of the anode fuel flow is ignored.
4) The cathode outlet air temperature is the same as the PEN average temperature. The large surface area of the fuel cell promotes substantial heat transfer between the cathode air and the fuel cell PEN.
5) Air flow is much larger than oxygen electrochemically reacted. This is reasonable because less than 25% of the oxygen is utilized for electrochemical reactions and 79% of the inlet air flow is nitrogen.
6) Fuel cell inlet temperature can be controlled (e.g., by means of recuperator bypass). In the system considered here, and that presented in Mueller et al. [20] the cathode inlet temperature is maintained within a few degrees through heat exchanger bypass manipulation.
7) Voltage responds instantaneously to the current step increase. The effects of species concentrations on voltage are assumed to be instantaneous relative to the slower fuel cell thermal response.
8) Gases have a constant average specific heat capacity. Because the fuel cell temperature must be maintained the average specific heat capacity will not change substantially.
9) All gases are ideal gases.

The situation considered in this analysis is of a pure hydrogen-air SOFC operating at steady state with constant air inlet temperature (T_{in}) and variable outlet temperature (T_o). At time $t = 0+$ the current is instantaneously increased to a constant value and the voltage instantaneously decreases due to increased polarizations, which

produce additional heat in the fuel cell. The cathode inlet temperature is kept constant by recuperator bypass manipulation (see Mueller et al. [7,18] for example). The air flow does not increase, to maintain a constant average fuel cell temperature, for a given amount of time. During the delay in air flow actuation to cool the fuel cell, the temperature within the fuel cell increases as extra heat is generated within the fuel cell following the current increase without additional air to further cool the fuel cell.

During the zero-order flow delay ($0+ < t < \tau_{air}$), following the load increase, fuel cell energy conservation can be expressed as:

$$mC\frac{dT_{out}}{dt} = \dot{N}_{air}C_p(T_{in} - T_{out}) + i\left(\frac{h_f}{nF} - V\right) \quad (6)$$

where m is the tri-layer mass, C is the tri-layer solid specific heat capacity; C_p is the air constant pressure specific heat capacity. Note that following the current increase and during the flow delay ($0+ < t < \tau_{air}$), the current, air flow, inlet temperature and voltage are all constant. Before the current step increase, the initial air flow is:

$$\dot{N}_{air} = \frac{i_\alpha((h_f/nF) - V_o)}{C_p(T_o - T_{in})} \quad (7)$$

where i_α is the initial current, V_o is the initial voltage, and T_o is the initial fuel cell cathode exit temperature.

The conservation of energy equation can be non-dimensionalized using the following non-dimensional parameters:

$$\bar{t} = \frac{t}{\tau_{air}}, \quad \Phi = \frac{i}{i_\alpha}, \quad \Theta = \frac{T_{out} - T_{in}}{T_o - T_{in}}, \quad \Psi = \frac{(h_f/nf) - V}{(h_f/nf) - V_o} \quad (8)$$

where $\bar{t}$ is non-dimensional time based upon τ_{air} is the fuel cell air zero-order flow delay, Φ is the current step increase based on i_α the initial current, Θ is the non-dimensional temperature based on the initial temperature difference between the fuel cell inlet (T_{in}) and outlet temperature (T_{out}), and Ψ is the non-dimensional voltage decrease from thermal maximum voltage (h_f/nF) based on the initial voltage (V_o).

Following the current manipulation the following non-dimensional energy conservation equations can be developed:

$$\frac{d\Theta}{d\bar{t}} = \frac{\dot{N}_{air}\tau_{air}C_p}{mC}\left(-\Theta + \Phi\Psi\frac{i_\alpha((h_f/nF) - V_o)}{\dot{N}_{air}C_p(T_o - T_{in})}\right) \quad (9)$$

where from the airflow requirement $\frac{i_\alpha((h_f/nF)-V_o)}{\dot{N}_{air}C_p(T_o-T_{in})} = 1$ and the non-dimensional grouping $Mu_T = \dot{N}_{air}\tau_{air}C_p/mC$ appears. Mu_T represents the ratio of thermal capacitance from the gas flow during the flow delay to the thermal capacitance of the fuel cell solid. Note that the air flow rate is constant during the delay, such that $\dot{N}_{air}$ in Mu_T is the air flow prior to the current perturbation. Identifying the grouping (Mu_T), the following simple differential equation results:

$$\frac{d\Theta}{d\bar{t}} = Mu_T(-\Theta + \Phi\Psi) \quad (10)$$

Eq. (10) can be solved with initial non-dimensional temperature $\Theta_o = 1$, as follows:

$$\Theta = (1 - \Phi\Psi)\exp(-Mu_T\bar{t}) + \Phi\Psi \quad (11)$$

The maximum fuel cell temperature will take place in the fuel cell just prior to the cathode compartment realization of the air flow increase ($\bar{t} = 1$). Therefore, it is possible to solve for Φ such that the fuel cell temperature is consistently maintained below a maximum temperature Θ_{max}=$(T_{max} - T_{in})/(T_o - T_{in})$ during the transient, as follows:

$$\Phi = \frac{1}{\Psi}\frac{\Theta_{max}\ \exp(Mu_T) - 1}{\exp(Mu_T) - 1} \quad (12)$$

Eq. (12) represents the extent to which the fuel cell current can be changed to maintain fuel cell temperature deviations below a maximum during the time of a zero-order air flow actuation delay. A voltage model can be developed to determine $\Psi(V)$ as a function of $\Phi(i)$. However, considering $\Psi = 1$, and defining $r = \Theta_{max}$ the equation is similar to that of the fuel depletion limitation, making it possible to compare current limitations due to fuel depletion to those due to temperature deviation constraints. In the two non-dimensional equations representing fuel depletion and temperature deviation transient limitations, Mu represents the ratio of the inlet flow capacitance during a delay (i.e., fuel flow into the fuel cell and thermal capacitance of the air flow through the fuel cell during the delay) to the capacitance internal to the fuel cell (i.e., fuel already within the volume of the fuel cell and fuel cell solid thermal capacitance). With respect to Mu (defined differently for fuel or thermal analysis) the intrinsic fuel cell transient performance to avoid fuel depletion and to maintain a given temperature deviation is represented by essentially the same non-dimensional equation. Mu is the non-dimensional number that governs fuel limitations to transient performance whereas Mu_T is the non-dimensional number that governs thermal limitations to transient performance.

4. Analytical results

Eqs. (5) and (12) are plotted in Fig. 2 to evaluate the extent to which SOFC fast electrochemical transient capability has to be constrained to maintain safe operating fuel cell conditions. In general, SOFC intrinsic load following capability depends upon the operating condition and flow delays, as well as the capacitance (species and thermal) of the fuel cell. The non-dimensional number Mu quantifies the thermal and species capacitance of the fuel cell. In the limit that Mu becomes 0 the fuel cell will have infinite load following. On the other hand in the limit that Mu goes towards infinity the allowable current increase becomes directly proportional to the extent to which the fuel utilization or temperature can change.

$$\frac{i_{max}}{i_1} \propto \lim_{Mu \to \infty}\left(\frac{r\ \exp(Mu) - 1}{\exp(Mu) - 1}\right) \propto r \quad (13)$$

The shorter the fuel and air flow delay the better the load following. With shorter flow delay fuel and air reaches the fuel cell more rapidly. Consequently, the period in which the current may have to be limited will be shorter, and higher current increases can be sustained during the delay. Similarly, the more capacitance (both thermal and electrochemically active species capacitance) within the fuel cell, the better the system load following capability will be. Furthermore, the SOFC systems will have better transient operating

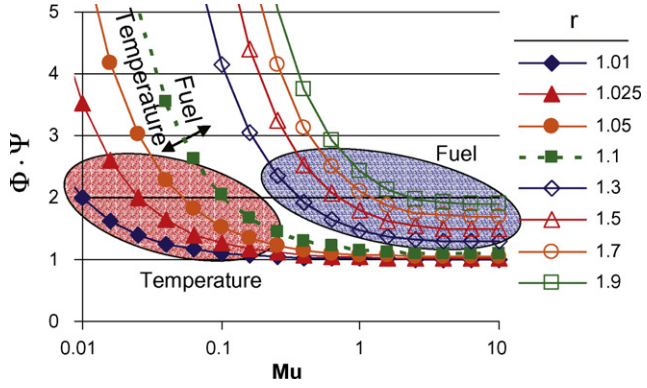

Fig. 2. Plot representing the theoretical extent that the fuel cell current can be changed such that a maximum utilization as well as a maximum temperature deviation from nominal is maintained during the time of a zero-order fuel and air flow delay.

Table 1
Values used in sample calculation of non-dimensional analysis.

τ_{ref}	1 s	Reformer flow delay time constant
τ_{air}	6 s	Air flow delay time constant
i_α	30 C s^{-1}	Initial current
$\bar{U}$	0.85	Initial fuel utilization
N	PV/RT	Molar capacity of anode
U_{max}	0.95	Maximum fuel utilization
P	1 atm	Pressure
V	0.005 m × 0.1 m × 0.1 m	Anode volume
T	1000 K	Temperature
$\dot{N}_{air}$	i_α/nFU_{O_2}	Initial air flow rate
U_{O_2}	0.2	Initial oxygen utilization
C_p	33.05 J mol^{-1} K^{-1}	Air specific heat capacity
C	800 J kg^{-1} K^{-1}	Fuel cell specific heat capacity
V_o	0.8 V	Initial voltage
V	0.6 V	Final voltage
T_{max}	1152 K	Maximum fuel cell temperature
T_o	1150 K	Initial fuel cell temperature
T_{in}	1000 K	Fuel cell inlet air temperature

capabilities at low power levels. At higher power operation (higher fuel cell currents), fuel cell electrochemically active species will be depleted quicker and the fuel cell temperature will increase more rapidly.

4.1. Fuel depletion

Sample calculations of Mu, r and Φ were made for fuel depletion within the fuel cell for typical operating conditions as shown in Table 1.

$$\begin{aligned} \mathrm{Mu} &= \frac{\tau_{ref} i_\alpha}{\bar{U} N n F} \approx 0.3 \\ r &= \frac{U_{max}}{\bar{U}} = \frac{0.95}{0.85} = 1.12 \\ \Phi &= \frac{i}{i_\alpha} = \frac{r\ \exp(\mathrm{Mu}) - 1}{\exp(\mathrm{Mu}) - 1} \approx 1.46 \end{aligned} \tag{14}$$

Generally, fuel cells are operated at near the maximum fuel electrochemical utilization to maintain high efficiency. However, fuel utilization can be decreased to improve the transient capability of fuel cells. Generally the ratio of max to operating fuel utilization ranges from approximately 1.1 to 1.9. Mu is generally greater then 0.2. Such a range is highlighted in Fig. 2.

From Fig. 2 it can be seen that If Mu is less than 2.5, the fuel cell capacitance can be used to improve transient performance capabilities. That is the amount of hydrogen within the fuel cell can improve the performance of the fuel cell. If Mu is larger than 2.5, the amount of capacitance within the fuel cell is relatively small compared to the consumption of hydrogen from the current and the capacitance within the fuel cell will not provide noticeable transient performance flexibility beyond what can be provided by balance-of-plant actuation.

From Eq. (5), it is possible to solve for Mu as a function of Φ and r, to ensure that the fuel cell fuel utilization is maintained for a given current increase:

$$\mathrm{Mu} \leq \ln\left[\frac{1-\Phi}{r-\Phi}\right] \tag{15}$$

For the current to be doubled without limitation (with $r = 1.12$ as used above) the species Mu should be approximately less than 0.1. Comparing this to the typical values of Mu = 0.3 suggests that fuel depletion can impose a severe limitation on SOFC transient capabilities. For the sample numbers provided, the flow delay would need to be reduced to 0.33 s to avoid fuel depletion limitations:

$$\tau_{ref} = \frac{\mathrm{Mu} U_o (PV/RT) nF}{i_o} \tag{16}$$

The non-dimensional analysis provides a simple closed-form solution to evaluate the load following capability of a particular fuel cell. If a certain transient performance is desired, it is possible to evaluate the required fuel utilization margin, reformer flow delay, or anode compartment size needed to achieve the given performance. Depending upon the initial fuel cell operating condition the non-dimensional equation further indicates if hydrogen stored within the fuel cell can provide load following improvement. The equation is simple and provides significant SOFC system transient performance insights.

4.2. Temperature deviation

Sample calculations of Mu_T, Θ_{max}, Ψ and Φ_T were conducted to compare the intrinsic load following limitations of fuel depletion and temperature deviation constraints as shown in Table 1.

$$\begin{aligned} \mathrm{Mu} &= \frac{\dot{N}_{air} \tau_{air} C_p}{mC} \approx 0.004 \\ \Theta_{max} &= \frac{T_{max} - T_{in}}{T_o - T_{in}} = 1.013 \\ \Psi &= \frac{(h_f/nf) - V}{(h_f/nf) - V_o} \approx \frac{1.25\,\mathrm{V} - 0.6\,\mathrm{V}}{1.25\,\mathrm{V} - 0.8\,\mathrm{V}} \approx 1.44 \\ \Phi &= \frac{i}{i_\alpha} = \frac{1}{\Psi} \frac{\Theta_{max}\ \exp(\mathrm{Mu}) - 1}{\exp(\mathrm{Mu}) - 1} \approx 3 \end{aligned} \tag{17}$$

Mu is generally much smaller for the temperature deviation constraint. Because the thermal Mu is generally much smaller than the fuel depletion Mu, the transient capability of fuel cells is generally not nearly as much limited by temperature deviation constraints. As is demonstrated by the sample calculation, it is theoretically possible to control the PEN temperature within a few degrees even for large load increases. For a reasonable load increase, such as doubling the current, it should be possible to control the PEN temperature to within a degree.

Air flow delay does not limit fuel cell performance as significantly as fuel processor flow delays due to the large thermal capacitance of the fuel cell. Physically the fuel cell thermal response is long (order of minutes to hours) compared to the more rapid fuel depletion (order of seconds). Considering the power required for air manipulation is generally a parasite on the system power, the analysis indicates it maybe possible to delay air for a few seconds to improve the system load following capability of the system (see [7,18]) with minimal effects on the fuel cell temperature response. The effects of blower power actuation delay can be quantified by moving horizontally to the right in Fig. 2 for a given load increase.

Fuel flow actuation delay can substantially limit fuel cell transient capability, if measures are not taken in system operation or design. On the other hand, the analysis indicates that due to large fuel cell thermal capacitance, fuel cell temperature can be closely controlled by manipulating the air flow through the fuel cell. The flexibility exists to temporarily delay air flow manipulation to improve the system transient performance with only small effects on the fuel cell temperature response. The analysis indicates one key bottleneck (fuel depletion) and one opportunity (thermal management) in the transient operation of integrated SOFC systems.

5. Fuel compensation

As illuminated by the non-dimensional analysis above, fuel flow delay to the fuel cell can be a principle fuel cell system transient performance limitation. To avoid fuel depletion during fuel processor transients or disturbances, the rate of fuel cell electrochemical reactions may have to be curtailed. As explored by Gaynor et al. [12] this can be accomplished by limiting the fuel cell current based

upon model predictive control or by maintaining a minimum fuel cell voltage.

It is however not desired to limit the fuel cell current to avoid fuel depletion. The analysis conducted indicates that to increase fuel depletion margins (1) the fuel utilization can be decreased, (2) the anode compartment size can be increased, (3) the operating pressure can be increased or (4) the fuel flow delay can be decreased. Each of the approaches has different costs and benefits.

Generally the most effective measure is to improve the rate at which the fuel can be delivered to the fuel cell. One interesting method to mitigate fuel depletion limitation in natural gas or biogas SOFC system is fuel compensation. In natural gas or biogas SOFC systems, the most significant fuel flow delay is due to pressure transients in the fuel processing system. It has been established by Beckhaus et al. [21] and Pukrushpan et al. [22] that fuel processor flow delays can be represented by dynamic resolution of the pressure using the dynamic orifice flow equations:

$$\frac{dP_{out}}{dt} = \frac{RT}{V}\left(\dot{N}_{in} - \dot{N}_{out} + \sum R\right) \tag{18}$$

$$\dot{N}_{out} = \dot{N}_o\sqrt{\frac{P_{in} - P_{out}}{\Delta P_o}} \tag{19}$$

A lead compensator can be implemented to the system inlet fuel flow to minimize the reformer flow delay. By "flooding" the reformer, pressure transients that limit the reformer outlet flow can be dramatically mitigated. The previous analysis indicates an exponential increase in transient capability with fuel processing flow delay decreases (see Eq. (4) and Fig. 2) motivating fuel flow compensation of fuel processor and delivery dynamics.

The following four steps can be taken to develop an open loop fuel flow compensator to demonstrate this concept: (1) find a representative fuel cell inlet flow transfer function $G_r(s)$, (2) determine a transfer function $G_d(s)$ with the desired response (i.e., with shorter delay), (3) compensate the system inlet flow by the factor $G_c(s) = G_d(s)/G_r(s)$, and (4) evaluate whether the compensated system responses are acceptable.

To demonstrate, a lead flow compensator is developed and implemented in the 5 kW SOFC system presented in Mueller et al. [7]. The system is a standalone integrated simple-cycle SOFC system comprised of a SOFC stack, natural gas steam reformer, anode-off gas combustor, blower and heat exchangers.

The first step to develop the compensator is to determine a representative simple fuel processor flow transfer function. This was done by comparing the fuel cell system that contains a non-linear orifice flow delay and reformation chemical kinetics fuel cell inlet fuel flow transient response to that of a first-order transfer function. A good transfer function for the fuel cell fuel flow response to a system inlet flow rate set-point change was found to be:

$$G_r(s) = \frac{4.8}{1.5\ s + 1} \tag{20}$$

Comparison of the complete system model dynamic response to a system inlet flow step increase perturbation to the first-order flow delay is shown in Fig. 3. The first-order transfer function well predicts the physical fuel cell inlet fuel flow response of the integrated system model that resolves chemical kinetics and the non-linear dynamics of flow delay caused by orifices in the system.

In the non-dimensional analysis above, a zero-order flow delay was considered to achieve the simple closed form equation. In this section, however, reformer flow delays are shown to be well approximated by a first-order transfer function. Nonetheless, the insights of the non-dimensional analysis using a zero-order flow delay remain valid, and the solution is more conservative but of the same order of magnitude.

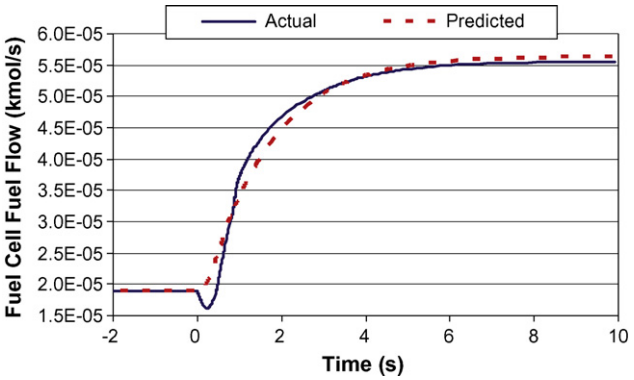

Fig. 3. Transfer function predicted fuel cell inlet fuel flow compared to the actual system fuel flow.

In the current system simulation, the system reformer flow delay is relatively large. Without compensation the fuel cell current has to be limited to avoid fuel depletion following a large current demand increase perturbation. From Eq. (16), it is possible to estimate a reformer delay such that the fuel cell performance will not have to be limited to avoid fuel depletion for a given magnitude of current demand increase perturbation. To ensure transient performance within system operating constraints, a desired reformer response time ($\tau_{desired}$), slightly faster than that determined from the non-dimensional analysis is implemented as follows:

$$G_d(s) = \frac{1}{\tau_{desired}\ s + 1} = \frac{1}{0.2\,s + 1} \tag{21}$$

From the reformer transfer function and desired reformer response, the system inlet fuel flow rate can be compensated to achieve the more desired reformer response characteristic by the following transfer function:

$$G_c(s) = \frac{G_d(s)}{G_r(s)} = \frac{\tau_{ref}\ s + 1}{\tau_{desired}\ s + 1} = \frac{1.5\,s + 1}{0.2\,s + 1} \tag{22}$$

The reformer transfer function gain (4.8 here), should not be included in the compensator transfer function as the gain represents the physical processes of the chemical reactions in the system.

The above open-loop compensator was implemented in the 5 kW simple cycle SOFC system model with non-linear flow delay. A 100 amp per second 22.4–67.0 amp current increase with and without fuel delay compensation was simulated. The system inlet fuel flow rate was manipulated proportionally to the current to maintain constant fuel cell fuel utilization. Ideally to maintain the fuel utilization within the fuel cell exactly, the fuel cell fuel flow rate would increase in proportion to the current. The fuel cell fuel flow, system

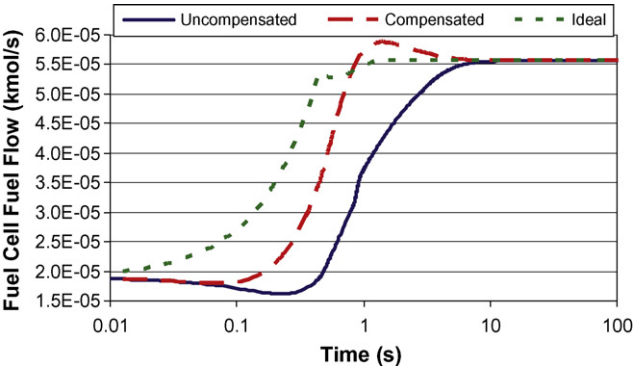

Fig. 4. 5 kW simple cycle system uncompensated, compensated and ideal constant fuel utilization fuel cell fuel flow response to a 100 amp per second 22.38–66.99 amp current increase.

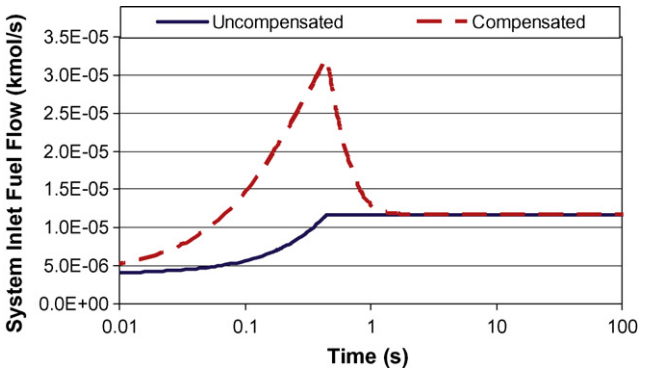

Fig. 5. 5 kW simple cycle system uncompensated and compensated system inlet fuel flow for a 100 amp per second 22.38–66.99 amp current increase.

inlet fuel flow, fuel cell exit fuel constituents, and fuel cell voltage responses to the current perturbation are presented in Figs. 4–6.

The uncompensated anode compartment inlet fuel flow response was delayed significantly (see Fig. 4). Due to the fuel delay the fuel cell current had to be limited to avoid fuel depletion. By implementing the flow compensator the anode compartment inlet fuel flow delay was significantly decreased. The compensated response approached the ideal constant utilization response, though not exactly. The increased performance of the compensated system is due to initially providing greater than steady-state reformer inlet fuel flow rate (see Fig. 5) in response to the perturbation. The fuel flow is initially three times larger than the steady-state fuel flow. The trade-of is that the more aggressive the desired response (i.e., shorter reformer delay), the greater the inlet fuel flow rate must be.

The fuel cell exit anode fuel constituents ($\Theta = X_{H_2} + X_{CO} + 4X_{CH_4}$) and cell voltage response are plotted in Fig. 6 for the uncompensated and compensated case. The compensated system fuel cell exit fuel constituents summed mole fraction remained above 0.08 and the voltage remained above 0.65 V during the transient. A more desired reformer delay of 0.2 s was found to be sufficiently fast to allow the current to be increased as demanded without limitation. In the uncompensated case the current had to be limited once fuel cell voltage dropped below 0.55 V per cell to avoid fuel depletion in the anode compartment. This result demonstrates that by understanding the intrinsic limitation of fuel depletion in load following, strategies can be implemented to avoid limitation imposed by fuel depletion to achieve rapid fuel cell load following.

6. Integrated system control demonstration

In addition to maintaining the fuel cell species concentrations and temperature within constraints, the combustor and reformer

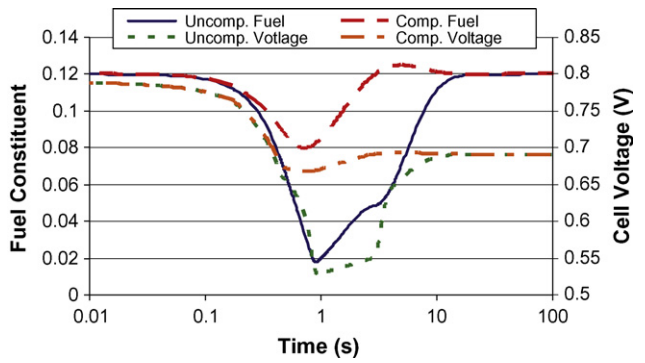

Fig. 6. 5 kW simple cycle system uncompensated and compensated system, fuel cell exit weighted fuel mole fraction and cell voltage response, to a 100 amp per second 22.38–66.99 amp current increase.

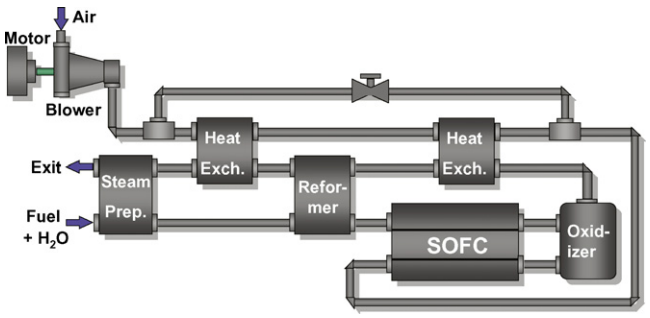

Fig. 7. Schematic of the 5 kW system simulated.

temperatures must also be maintained. In this section reformer temperature control, fuel flow control of the combustor, blower power control of the fuel cell temperature, and current control of the fuel cell power concepts are discussed and simulated to demonstrate the intrinsic load following capability of an SOFC system with appropriate controls.

6.1. Reformer temperature

The reformer temperature may or may not be controlled directly depending upon the design of the SOFC system. In the system considered here, shown in Fig. 7, reformer temperatures are maintained by a network of heat exchangers to sufficiently provide heat to the reformer. Prior simulations have indicated that the reformer temperature can be well maintained during transients due to the system thermal integration and thermal inertia of the fuel processor components [7].

6.2. Combustor temperature

Controlling the combustor temperature can be a challenge because combustor temperatures are a function of the combustor stoichiometry that can change very rapidly depending upon fuel and air transients and the extent of fuel cell electrochemical fuel utilization. In addition, the combustor generally has small thermal inertia (small mass). It is possible, however, to accurately control the combustor stoichiometry by manipulating the fuel flow, air flow and/or the fuel cell current. With fast fuel manipulation (e.g., using fuel flow compensation), it is possible to maintain sufficient fuel within the fuel cell and to actually manipulate the amount of fuel through the fuel cell to control the combustor temperature.

6.3. System power and fuel cell temperature

The fuel cell temperature can be effectively controlled by manipulating the air flow through the fuel cell. In the system considered the air through the fuel cell is varied by manipulating the blower shaft speed.

The non-dimensional analysis indicated that the air flow rate does not have to increase instantaneously to maintain close control of the fuel cell temperature. During short fuel cell system power demand transients, the blower can be temporarily manipulated (i.e., blower power reduced to increase system output power) to provide some load tracking buffer for the system. Such control concepts as developed in detail in Mueller et al. [7] was implemented in the current system.

6.4. System simulation

To demonstrate the intrinsically fast load following capability of an SOFC system, simulations were accomplished using (1) the

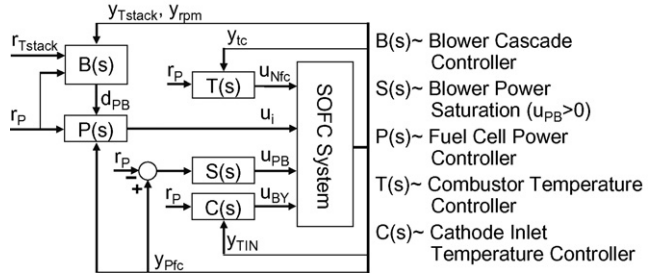

Fig. 8. Integrated controller with augmented fuel flow combustor temperature control and blower power buffering.

Table 2
Fuel flow combustor temperature and current power controller constants.

Fuel flow combustor temperature controller		
K_{tc}	5×10^{-8} kmol K^{-1}	Combustor temperature feedback gain
I_{tc}	1×10^{-9} kmol K^{-1}	Combustor temperature integral feedback gain
τ_{ref}	1.5 s	Reformer flow delay time constant
τ_{shape}	0.4 s	Compensated reformer delay time constant
Rate	+0.5 K s^{-1}	Combustor temperature set-point ramp rate
Sat.	0–80 A	Current saturation
Current fuel cell power controller		
K_{Pfc}	50 A kW^{-1}	Fuel cell power feedback proportional gain
I_{Pfc}	1 A kW^{-1}	Fuel cell power feedback integral gain
Sat.	0–80 A	Current saturation
Blower cascade controller		
r_{Tstack}	1150 K	Reference fuel cell operating temperature
K_{Tstack}	10,000 RPM K^{-1}	Temperature feedback proportional gain
KRPM	1×10^{-3} kW RPM^{-1}	Shaft speed feedback proportional gain
SAT	0–1.5 kW	Blower power saturation

fuel flow combustor temperature controller with compensation, (2) the fuel cell current controller for fuel cell power, and (3) the fuel cell thermal management controllers in the bulk 5 kW system (see Fig. 7). To help clarify input–output pairing and the control structure used, the overall integrated controller is presented in Fig. 8. Constants used in this new controller concept are presented in Table 2.

System responses to a rapid one kilowatt per second 2.4–4.8 kW load increase perturbation are shown in Fig. 9. The fuel cell voltage and the combustor temperature are maintained within 20 K.

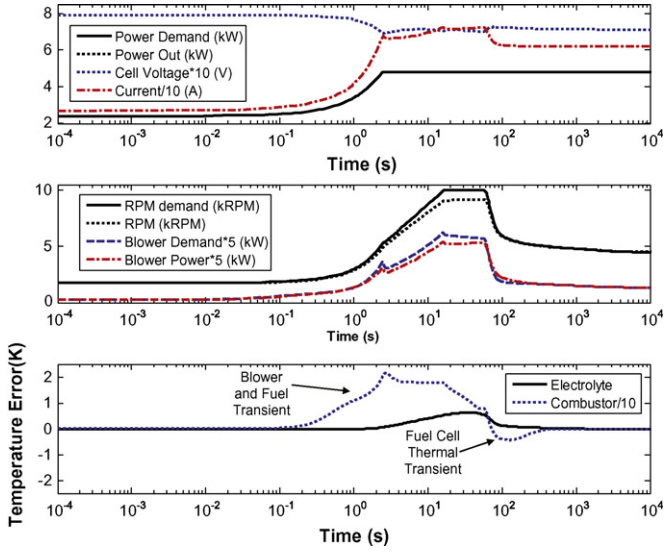

Fig. 9. A kilowatt per second 2.4–4.8 kW load increase with compensated fuel flow combustor temperature control, current fuel cell power control and blower power buffering.

The power ramp is tracked exactly with only slight blower power buffering of control actions. Slight variations in the blower power during the transient response did not significantly affect the fuel cell thermal response, as expected.

These results demonstrate exceptionally close control of the fuel cell temperature, and adequate control of the combustor temperature without fuel depletion in the anode compartment in response to a significant and rapid power demand increase. The nearly exact tracking of power demand within operating constraints demonstrates the intrinsic rapid transient capability of SOFC systems with careful control and rapid fuel flow manipulation.

7. Discussion and conclusions

A non-dimensional approach that quantifies the extent to which SOFC fast electrochemical response characteristics must be limited because of requirements to maintain fuel flow and temperature of the fuel cell has been derived. New non-dimensional groupings for fuel depletion, $(\tau_{ref} i_\alpha)/(\bar{U}NnF)$, and temperature deviation, $(\dot{N}_{air}\tau_{air}C_p)/(mC)$, constraints have been identified, representing the ratio of flow capacitance (electrochemical, thermal) to that of the fuel cell. With respect to such groupings the non-dimensional equations representing the extent to which current can be increased while avoiding fuel depletion and maintaining a given temperature deviation are similar.

The analyses indicate that fuel processor delay can significantly limit fuel cell load following capability, while SOFC system intrinsic load following capability is not severely limited by temperature constraints. For natural gas or biogas systems it is possible to manipulate the system inlet flow rates to compensate for flow transients within the system fuel processor. Such compensation makes it possible to maintain sufficient fuel within the anode compartment, avoiding the need to limit the fuel cell current to avoid fuel depletion during transients.

Analysis and system simulation indicate that cathode air exit temperature can be well controlled. Rapid SOFC load following should only be practiced if it does not reduce SOFC durability. Since it is possible to control both the inlet fuel cell temperature and fuel cell average temperature this should be possible with the current means to maintain close control of the fuel cell temperature distribution.

Intrinsically fast SOFC transient capability has been identified; however, some advanced control concepts to maintain SOFC temperature distribution during transients need further development for practical fuel cells to achieve such capabilities.

References

[1] M.C. Williams, J.P. Strakey, W.A. Surdoval, L.C. Wilson, Solid oxide fuel cell technology development in the U.S., Solid State Ionics 177 (19–25) (2006) 2039–2044.
[2] M.C. Williams, J. Strakey, W. Sudoval, U.S. DOE fossil energy fuel cells program, Journal of Power Sources 159 (2) (2006) 1241–1247.
[3] M.C. Williams, J.P. Strakey, S.C. Singhal, U.S. distributed generation fuel cell program, Journal of Power Sources 131 (1–2) (2004) 79–85.
[5] SECA wraps first phase with SOFCs on way to commercial reality. Fuel Cells Bulletin; 2007(7):4.
[6] Siemens SOFC system exceeds DOE objectives. Fuel Cells Bulletin; 2007(1): 5–6.
[7] F. Mueller, F. Jabbari, R. Gaynor, J. Brouwer, Novel solid oxide fuel cell system controller for rapid load following, Journal of Power Sources 172 (1) (2007) 308–323.
[8] F. Mueller, J. Brouwer, F. Jabbari, S. Samuelsen, Dynamic simulation of an integrated solid oxide fuel cell system including current-based fuel flow control, Journal of Fuel Cell Science and Technology 3 (2) (2006) 144–155.
[9] C. Stiller, B. Thorud, O. Bolland, R. Kandepu, L. Imsland, Control strategy for a solid oxide fuel cell and gas turbine hybrid system, Journal of Power Sources 158 (1) (2006) 303–315.
[10] F. Mueller, F. Jabbari, J. Brouwer, R. Roberts, T. Junker, H. Ghezel-Ayagh, Control Design for A Bottoming Solid Oxide Fuel Cell Gas Turbine Hybrid System, ASME, Irvine, CA, 2006.

[11] R. Kandepu, L. Imsland, B.A. Foss, C. Stiller, B. Thorud, O. Bolland, Modeling and control of a SOFC-GT-based autonomous power system, Energy 32 (4) (2007) 406–417.
[12] R. Gaynor, F. Mueller, J. Faryar, J. Brouwer, On control concepts to prevent hydrogen starvation in solid oxide fuel cells, Journal of Power Sources 180 (1) (2008) 330–342.
[13] Y. Inui, N. Ito, T. Nakajima, A. Urata, Analytical investigation on cell temperature control method of planar solid oxide fuel cell, Energy Conversion and Management 47 (15–16) (2006) 2319–2328.
[14] R. Roberts, J. Brouwer, F. Jabbari, T. Junker, H. Ghezel-Ayagh, Control design of an atmospheric solid oxide fuel cell/gas turbine hybrid system: Variable versus fixed speed gas turbine operation, Journal of Power Sources 161 (1) (2006) 484–491.
[15] A. Nakajo, C. Stiller, G. Harkegard, O. Bolland, Modeling of thermal stresses and probability of survival of tubular SOFC, Journal of Power Sources 158 (1) (2006) 287–294.
[16] C. Haynes, Simulating process settings for unslaved SOFC response to increases in load demand, Journal of Power Sources 109 (2) (2002)365–376.
[17] T. Kaneko, J. Brouwer, G.S. Samuelsen, Power and temperature control of fluctuating biomass gas fueled solid oxide fuel cell and micro gas turbine hybrid system, Journal of Power Sources 160 (1) (2006) 316–325.
[18] F. Mueller, R. Gaynor, A.E. Auld, J. Brouwer, F. Jabbari, G.S. Samuelsen, Synergistic integration of a gas turbine and solid oxide fuel cell for improved transient capability, Journal of Power Sources 176 (1) (2008) 229–239.
[19] Mitsubishi develops Japan's first SOFC-MGT system. Fuel Cells Bulletin; 2006(10):4.
[20] F. Mueller, F. Jabbari, R. Gaynor, J. Brouwer, Novel Solid Oxide Fuel Cell System Controller for Rapid Load Following, Journal of Power Sources 172 (1) (2007) 308–323.
[21] P. Beckhaus, A. Heinzel, J. Mathiak, J. Roes, Dynamics of H_2 production by steam reforming, Journal of Power Sources 127 (1–2) (2004) 294–299.
[22] T.J. Pukrushpan, G.A. Stefanopoulou, P. Huei, in: J.M. Grimble, A.M. Johnson (Eds.), Control of Fuel Cell Power Systems: Principles, Modeling, Analysis, and Feedback Design, Springer, London, 2005.